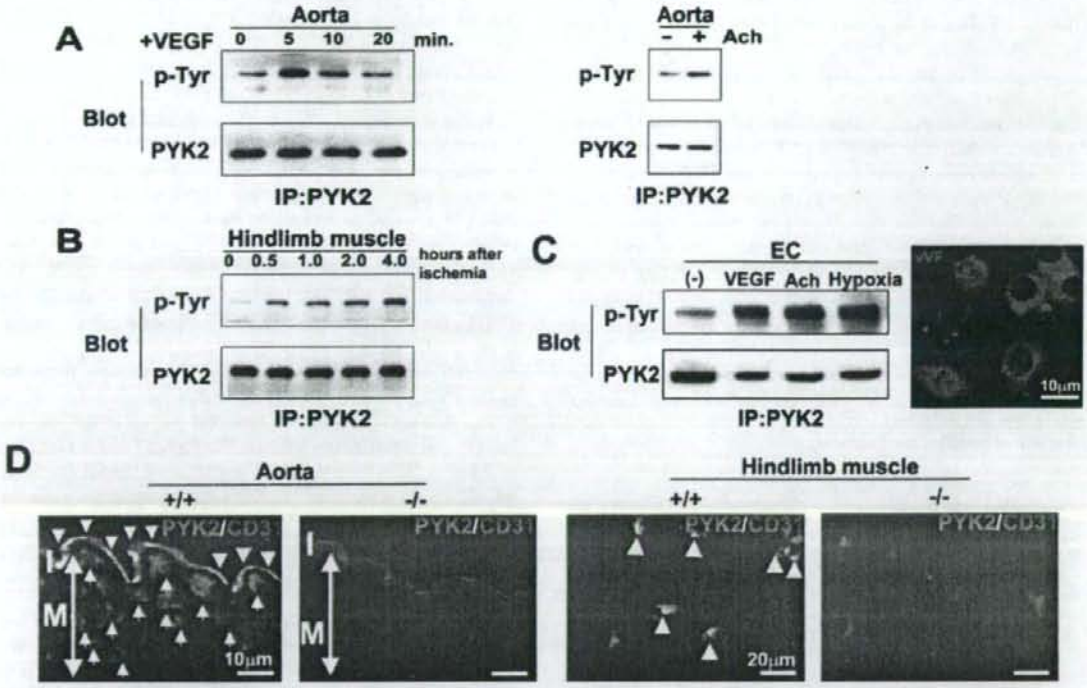

Figure 1. Activation of PYK2 by VEGF, Ach, and hind-limb ischemia. A, Aortic tissue removed from wild-type mice was incubated with the medium including VEGF (100 ng/mL) or Ach (1 μmol/L) for 5 minutes. B, Time-dependent PYK2 phosphorylation in hind-limb muscles was examined after ligation of femoral artery. C, Left, Aortic ECs were stimulated with VEGF (100 ng/mL) or Ach (1 μmol/L) for 5 minutes or exposure with 1% hypoxia for 18 hours. Tissue or cell lysates were subjected to immunoprecipitation with an anti-PYK2 antibody, followed by immunoblotting with anti-phosphotyrosine or anti-PYK2 antibodies. Data are mean±SE (n=5 each); representative results are shown. Right, Cells were immunostained with anti–von Willebrand factor antibody to identify the ECs. D, Distribution of PYK2 in the aorta and limb muscle. Aorta and limb muscle were frozen-sectioned, fixed with acetone, and subjected to double immunostaining with antibodies against PYK2 (green) and CD31 (red). The merged cells (yellow) are indicated by arrowheads; PYK2-positive smooth muscle in the aorta, by arrows. I indicates intima; M, media.

immunostaining with anti–phospho-^{1176}Ser-eNOS antibody whether VEGF-mediated phosphorylation of eNOS can be restored (Figure 2D). eNOS phosphorylation was observed in VEGF-exposed cells in which GFP-tagged PYK2 plasmid was transfected, whereas phospho-eNOS–positive cells were barely detected in the control GFP-transfected cells.

We next studied whether intracellular Ca^{2+} mobilization was influenced by PYK2 deficiency. Figure 3A shows that VEGF-mediated elevation of cytoplasmic Ca^{2+} levels was markedly inhibited in the PYK2-deficient ECs (Ca^{2+} concentrations in PYK2$^{-/-}$, 95±24 nmol/L versus wild type, 432±69 nmol/L; $P<0.001$), whereas Ca^{2+} mobilization with ATP that directly opens the Ca^{2+} channel on the plasma membrane[15] was comparable to the wild type (Figure 3A), suggesting that the pathway for the receptor-independent Ca^{2+} mobilization is not impaired. To study the effect of PYK2 deficiency on the other Ca^{2+} signaling pathway not involving NO formation, we studied the activation of the Ca^{2+}-dependent transcription factor nuclear factor of activated T cells 2 (NFATc2), which was shown to be crucial for VEGF-mediated angiogenesis.[16] The results showed that 68±8% of the wild-type cells showed nuclear translocation of NFATc2 from cytoplasm 30 minutes after VEGF stimulation, whereas in the PYK2-deficient cells, the translocation was markedly reduced (22±6%; $P<0.01$), indicating that PYK2 deficiency inhibits Ca^{2+} signaling pathway not involving NO formation (Figure 3B). To prove that the functional effects are due directly to the loss of PYK2, we transfected the GFP-tagged PYK2 plasmid to the PYK2-deficient cells and observed VEGF-mediated nuclear translocation of NFATc2. In the PYK2-deficient cells transfected with GFP-tagged PYK2 plasmid, the number of NFATc2-translocated cells increased significantly (from 22±6% to 48±9%; $P<0.05$; Figure 3B), whereas in the control GFP-transfected cells, the translocated cells did not increase significantly (data not shown). Pretreatment with a chelator of intracellular Ca^{2+} store, AM-BAPTA (5 μmol/L), in the Ca^{2+}-free medium for 45 minutes did not affect VEGF-induced Akt activation in ECs (Figure 3C), indicating that Akt activation is Ca^{2+} independent in our system.

Reduced Response by PYK2 Deficiency in NO Production and Ach-Mediated Vasodilatation

The intracellular NO level was measured with 4-amino-5-methyl-amino-2′,7′-difluorofluorescein diacetate (DAF-FM DA). NO was visualized as green under laser

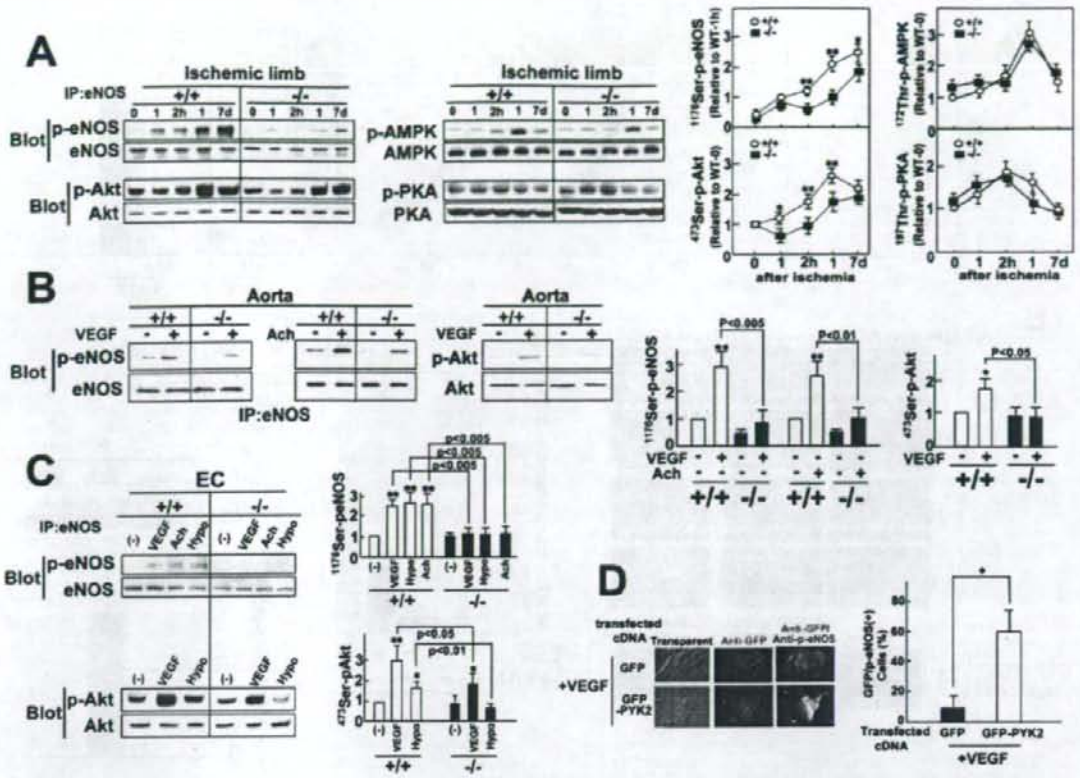

Figure 2. Impaired eNOS/Akt activation in PYK2-deficient mice. A, Skeletal muscle (n=10) was excised at the indicated time after ischemia. B, Aortic tissue (n=6 for each stimuli) was stimulated with VEGF (100 ng/mL) or Ach (1 μmol/L) for 5 minutes. C, Aortic ECs (n=6 for each stimuli) were stimulated with VEGF (100 ng/mL) or Ach (1 μmol/L) for 5 minutes or 1% hypoxia for 18 hours (n=6 each). Cell lysates were subjected to immunoprecipitation with anti-eNOS antibody, followed by immunoblot with antibodies against ^{1176}Ser-phosphorylated eNOS or eNOS. In addition, lysates were immunoblotted with antibodies against ^{473}Ser-phosphorylated Akt or Akt. Relative phosphorylation levels of eNOS and Akt are shown. Open circles and closed squares indicate the wild-type and PYK2$^{-/-}$ mice, respectively. A, $^{*}P<0.05$, $^{**}P<0.01$ vs the same time points of the PYK2$^{-/-}$ mice. B, C, $^{*}P<0.05$, $^{**}P<0.005$ vs the nonstimulated control. D, Aortic ECs were transfected with GFP- or GFP-PYK2-cDNA-plasmid. Forty-eight hours after transfection, cells were stimulated with VEGF (100 ng/mL), fixed with 4% paraformaldehyde, permeabilized with 0.02% Triton/PBS, and immunostained with antibodies against GFP- (red) or ^{1176}Ser-phosphorylated eNOS (green). Ratio of the GFP/p-eNOS double-positive cells (%) (yellow) to the total GFP-positive cells (red) was evaluated. $^{*}P<0.005$; n=4.

microscopy (Figure 4A). In the wild-type ECs, VEGF increased NO levels by 3.2-fold ($P<0.005$ versus untreated cells), whereas this increase was severely impaired in the PYK2-deficient ECs. NO metabolites in the 24-hour urine sample were significantly lower in the PYK2$^{-/-}$ mice than the wild-type mice (4084±820 versus 9326±1163 nmol; $P<0.005$; Figure 4B). Oral administration of N^{G}-nitro-L-arginine methyl ester (L-NAME; 3 mmol/L in drinking water) to the wild-type mice reduced the NO metabolite production to a level comparable to the PYK2$^{-/-}$ mice (Figure 4B).

Ach-mediated vasodilatation is induced by the eNOS-NO system. We next examined whether Ach-mediated relaxation of the aorta is influenced by PYK2 deficiency. The dose-dependent relaxation of the isolated aorta constricted by norepinephrine was evaluated (Figure 4C). Ach (10 μmol/L) -mediated relaxation response was much weaker in the PYK2-deficient aorta than in the wild-type aorta (32±8% versus 59±5% relaxation; $P<0.01$), whereas norepinephrine (300 nmol/L) -mediated vasoconstriction in the PYK2-deficient aorta did not significantly differ from the wild-type aorta (190±30% versus 165±6% relative to 50 mmol/L KCl–mediated constriction; n=5). This result suggests that Ca^{2+} signaling transmitted mainly through voltage-dependent Ca^{2+} channel leading to the constriction of vascular smooth muscle cells is not impaired in the PYK2-deficient aorta.

To evaluate the NO dependency on Ach-mediated vasorelaxation, the effect of L-NAME was studied. Addition of L-NAME (10 μmol/L) markedly suppressed the Ach-mediated maximum relaxation of the wild-type aorta (from 59±5% to 17±2%; $P<0.001$; n=4), whereas in the PYK2-deficient aorta, the reduced relaxation response was suppressed further to a level comparable to L-NAME–treated

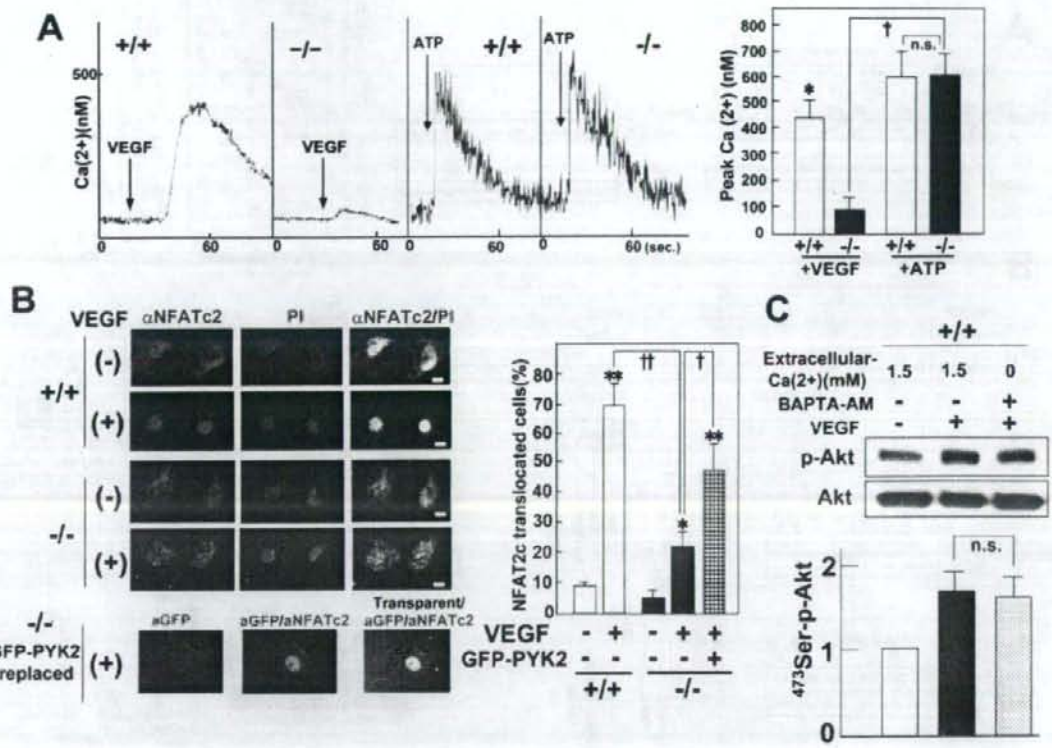

Figure 3. Impaired Ca^{2+} mobilization in PYK2-deficient mice. A, VEGF (100 ng/mL) - or ATP (1 mmol/L) -mediated cytoplasmic Ca^{2+} concentrations were measured in Fura-2–loaded ECs by a fluorescence microscope (n=12 each). †$P<0.001$, *$P<0.001$ vs VEGF-stimulated $PYK2^{-/-}$ cells. B, Top, ECs were fixed with 4% paraformaldehyde 30 minutes after VEGF stimulation, treated with 0.05% triton, and immunostained with anti-NFATc2 antibodies and propidium iodide (PI). Bottom, PYK2-deficient ECs were transfected with GFP-tagged PYK2 plasmid. Forty-eight hours after transfection, cells were stimulated with VEGF for 30 minutes and immunostained with anti-NFATc2 and anti-GFP antibodies. The number of cells in which NFATc2 was translocated to the nucleus was counted and shown relative to total plated cell numbers (n=4 in each experiment). *$P<0.05$, **$P<0.005$ vs nonstimulated control cells. †$P<0.05$, ††$P<0.01$. Scale bar=10 μm. C, After serum starvation (0.5% FBS) for 16 hours, cells were preincubated with BAPTA-AM (5 μmol/L) in the Ca^{2+}-free medium for 45 minutes and subsequently stimulated by VEGF for 5 minutes. Lysates were subject to immunoblot by antibodies against Akt and ^{473}Ser-phosphorylated Akt.

wild-type aorta (from 32±8 to 18±3%; $P<0.005$; n=4). These findings indicate that Ach-mediated vasorelaxation depends mainly on NO production, in which an involvement of PYK2-mediated NO signaling was estimated to be ≈64% [(59−32/59−17)×100] of the total NO-mediated vasodilation activated downstream of Ach. NO donor (nitroprusside) –induced vasorelaxation of the aorta was similar in both groups (82±4 versus 83±4%; n=5), suggesting that NO-mediated signal transduction for vasodilatation is not impaired in the PYK2-deficient aorta (Figure 4C).

NO-mediated vasodilatation requires cGMP as a second messenger. We therefore measured the amount of cGMP in the aorta. Basal cGMP production in the $PYK2^{-/-}$ mice was 41% lower than that in the wild-type mice. Ach increased aortic cGMP production 4.8-fold in the wild-type mice, whereas the increase in the $PYK2^{-/-}$ mice was 2.0-fold, significantly ($P<0.01$) lower than in the wild-type mice (Figure 4D).

Decrease in Neovessel Formation by PYK2 Deficiency

Angiogenesis in the ischemic tissue requires eNOS activation.[17] We analyzed the blood flow recovery and neovessel formation after hind-limb ischemia. The ratio of blood flow recovery assessed by laser Doppler imaging was significantly lower in the $PYK2^{-/-}$ mice than in the wild-type mice (50% versus 76% recovery at 3 weeks after ischemia; $P<0.01$; Figure 5A). Oral administration of L-NAME (3 mmol/L in drinking water) significantly reduced the recovery ratio in the wild-type (from 76% to 62%; $P<0.05$) and $PYK2^{-/-}$ (from 50% to 37%; $P<0.05$) mice (Figure 5A). Considering that the recovery ratio of the L-NAME–treated wild-type mice (62%) is close to that of the $PYK2^{-/-}$ mice (50%), the blood flow recovery after hind-limb ischemia is considered to be regulated mainly by PYK2-mediated NO signaling. We also counted the number of $CD31^+$ vessels in the ischemic muscle. There was no significant difference in the basal vessel

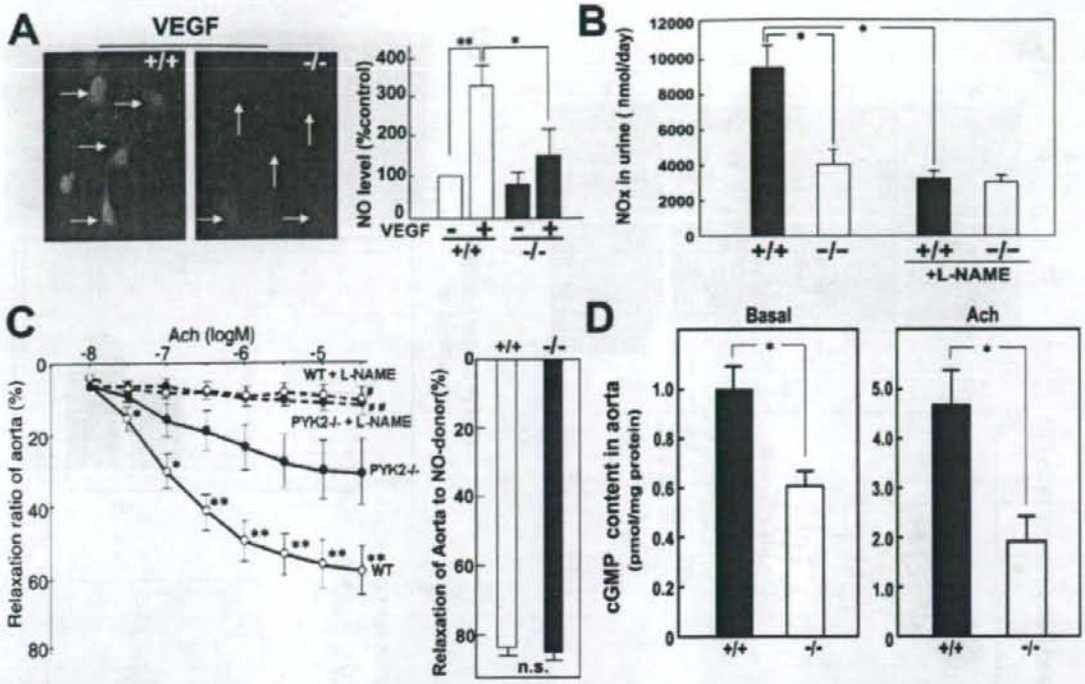

Figure 4. PYK2 effects on NO production and Ach-mediated vasodilatation. A, Measurement of the intracellular NO level. ECs were loaded with DAF-FM DA (10 μmol/L), and NO was visualized as green under laser microscopy. The average intensities in the ECs relative to the control group were evaluated. *P<0.01, **P<0.005 (n=8 each). B, NO production assessed by NO metabolites in the 24-hour urine sample was evaluated in the mice treated or untreated with L-NAME (3 mmol/L) for 7 days. Data are mean±SE (n=6). *P<0.005. C, Ach- and NO donor– (nitroprusside) mediated vasodilation in the aorta constricted by norepinephrine (100 nmol/L). Ach (10 nmol/L to 100 μmol/L) -mediated or nitroprusside (10 μmol/L) relaxation in the Tyrode's solution with or without L-NAME (10 μmol/L) was assessed by percent relaxation relative to papaverine (100 μmol/L) -mediated relaxation (100%). *P<0.05, **P<0.01 vs the same concentration of the PYK2$^{-/-}$ mice; #P<0.001 vs the maximum concentration of the wild-type mice; ##P<0.005 vs the maximum concentration of the PYK2$^{-/-}$ mice. D, cGMP contents in tissue lysates from untreated (basal) or Ach (1 μmol/L) -stimulated aorta were measured with an enzyme immunoassay kit. *P<0.01. Data are mean±SE (n=4 each); representative results are shown.

numbers surrounding the muscle fibers. The vessel number (per muscle fiber) in the wild-type mice increased 2.3-fold (P<0.005) after hind-limb ischemia, whereas the PYK2$^{-/-}$ mice showed no significant increase (Figure 5B).

We next examined whether PYK2 deficiency affects the mobilization or differentiation of EPCs. We found that 3 days after limb ischemia, the number of circulating CD45^{-}/Flk-1^{+} EPCs was significantly lower (36%; P<0.05) in the PYK2$^{-/-}$ mice than the wild-type mice (0.28±0.06% and 0.18±0.03% relative to total peripheral blood mononuclear cells, respectively; n=10 each; Figure 5C). Considering that the mobilization of EPCs was reportedly regulated by the eNOS function of EPCs in a VEGF-dependent manner,[18] the present study suggests that PYK2 deficiency attenuates VEGF-mediated EPC mobilization by impairing Ca^{2+}/eNOS signaling.

Impaired cGMP-Dependent Protein Kinase– and eNOS-Mediated Migration of PYK2-Deficient ECs

NO-mediated angiogenesis depends on the migration of ECs, in which cGMP-dependent protein kinase (GK) or eNOS plays a crucial role.[19] Because it was reported that the migration of macrophages was severely impaired in PYK2$^{-/-}$ mice,[11] the migration activity of aortic ECs was evaluated by the Boyden chamber assay. VEGF-mediated migration was 41% lower (P<0.01) in the PYK2-deficient ECs than wild-type ECs (Figure 6A). Pretreatment with L-NAME (3 mmol/L) or Rp-8-Br-cGMPS (1 μmol/L, a GK inhibitor) markedly inhibited the VEGF-mediated migration activities of wild-type ECs (50% and 45% inhibition, respectively; Figure 6A). L-Arginine (1 mmol/L) or GK activator 8-Bromo-cGMP (1 μmol/L) treatment restored the reduced migration of PYK2-deficient ECs to the wild-type level, whereas L-NAME or GK inhibitor (1 μmol/L) did not significantly affect their migration activities (Figure 6A).

The tubular formation activity and 3-dimensional angiogenesis in the Matrigel plug were significantly decreased in the PYK2-deficient ECs (59% and 38% decrease, respectively; Figure 6B and 6C). L-NAME diminished the tubular formation of wild-type ECs (39%; P<0.05), and L-arginine treatment improved the decreased activity of PYK2-deficient ECs (52%; P<0.01) (Figure 6B). These findings suggested that PYK2-mediated migration of ECs and angiogenic response are regulated mainly by NO and GK activation.

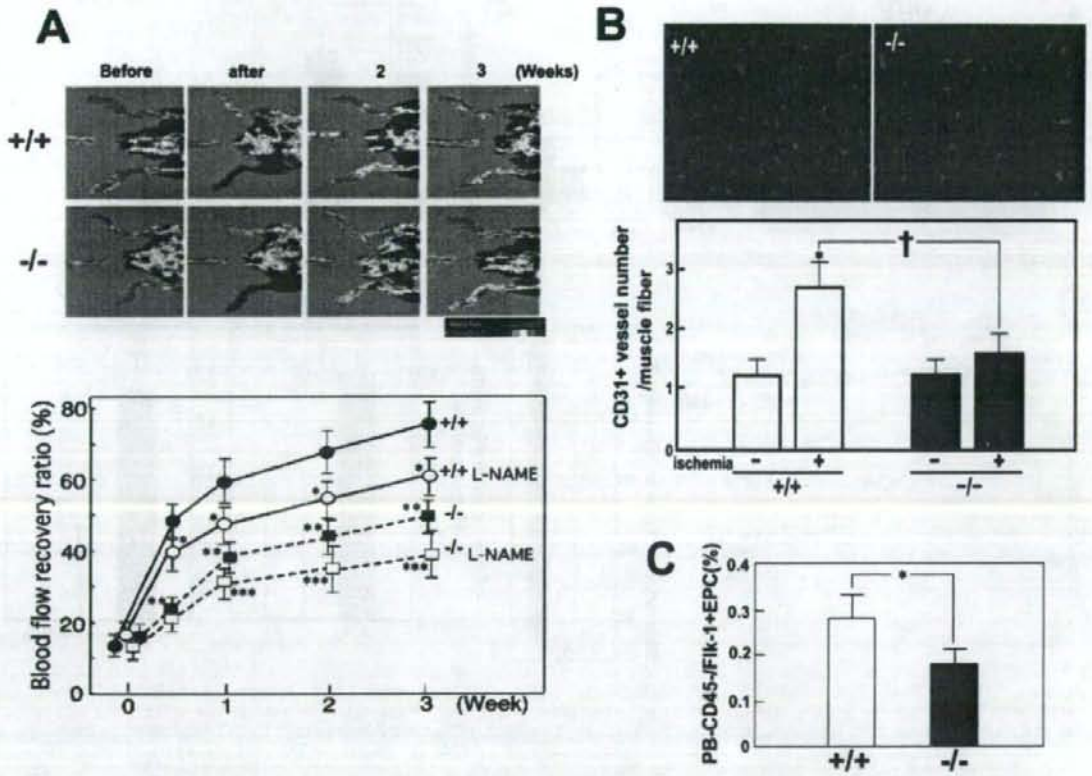

Figure 5. Reduced recovery of blood flow and neovessel formation in the ischemic hind limb of PYK2$^{-/-}$ mice. A, Reduced blood perfusion in ischemic limbs (green to blue) was observed in the PYK2$^{-/-}$ mice in contrast with perfusion (red to yellow) in the wild-type mice. Computer-assisted analyses revealed significantly lower blood perfusion values in PYK2$^{-/-}$ mice. Administration of L-NAME (3 mmol/L) in drinking water reduced the increased perfusion in both the wild-type and PYK2$^{-/-}$ mice. Values shown are mean±SE (n=8 each time point). *P<0.05, **P<0.01 vs wild-type mice; ***P<0.05 vs PYK2$^{-/-}$ mice. B, Hind-limb muscles were removed 14 days after ischemia, and ECs were immunostained with an anti-CD31 antibody. The number of CD31$^+$ vessels surrounding the muscle fiber is shown. Data are mean±SE (n=8 each). *P<0.005 vs ischemia (-) muscles; †P<0.005. C, Three days after hind-limb ischemia, peripheral blood was incubated with FITC-conjugated anti-CD45 and PE-conjugated anti-Flk-1 antibodies. Peripheral blood–derived mononuclear cells were analyzed by fluorescence-activated cell sorter after lysis of erythrocytes. The relative number of CD45$^-$/Flk-1$^+$ EPCs to total mononuclear cells was shown (n=10; *P<0.05).

Considering that GK affects the cytoskeleton structure,[20] PYK2 may modulate the cytoskeleton structure, leading to the regulation of cell migration and eventually angiogenesis. We therefore examined the effect of PYK2 on the F-actin structure of ECs. In the basal condition, we observed the stress fibers in 55±5% of the total wild-type ECs attaching on a fibronectin-coated dish and in 76±5% of PYK2-deficient ECs (P<0.05) (Figure 7A). VEGF stimulation markedly decreased the number of stress fiber–positive wild-type cells (from 55±5% to 15±4%; P<0.01) and 64±6% of the total attaching wild-type cells exhibited the accumulation of F-actin at the plasma membrane, whereas in the PYK2-deficient ECs, 72±8% of cells still had the apparent stress fibers and the cells showing the F-actin accumulation at the plasma membrane was only 23±3%. Pretreatment with L-NAME inhibited VEGF-mediated F-actin accumulation at the plasma membrane (P<0.01) and increased the stress fiber formation (P<0.05) in the wild-type cells, whereas the addition of L-arginine to PYK2-deficient ECs attenuated the stress fiber formation (P<0.01) and enhanced the VEGF-mediated F-actin accumulation at the plasma membrane (P<0.05).

Because F-actin structure was regulated by Rho-family small GTPases, we evaluated the activities of RhoA and Rac1 by pull-down assay using GST-RBD[21] and GST-PBD,[22] respectively (Figure 7B). The amount of GTP-bound RhoA was decreased significantly in the wild-type ECs 5 minutes after VEGF treatment, whereas in the PYK2-deficient ECs, they were reduced more extensively than in the wild-type ECs. In contrast, the amount of GTP-bound Rac1 was increased markedly in the wild-type ECs, whereas its increase was abolished by the PYK2 deficiency. Considering that Rac1 plays a pivotal role in F-actin reorganization[23] and PYK2 promotes Rac-mediated JNK activation,[24] lack of VEGF-mediated Rac1 activation may be associated with the altered F-actin structure in the PYK2-deficient cells. Further-

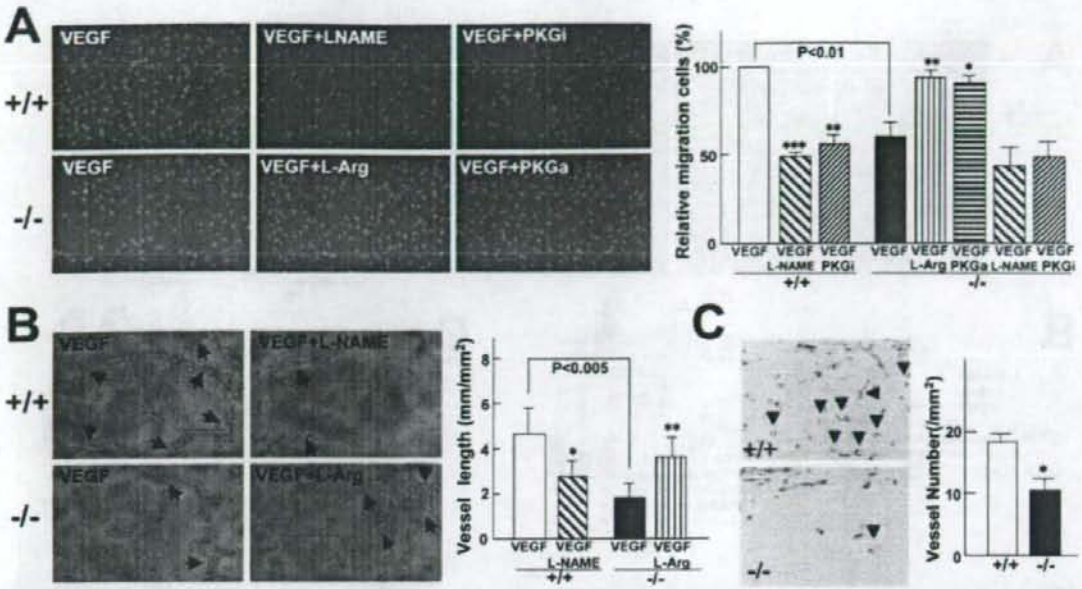

Figure 6. Decrease in GK- and eNOS-dependent migration of PYK2-deficient ECs. A, VEGF-mediated migration of ECs was evaluated with GK inhibitor (PKGi; 1 μmol/L Rp-8-Br-cGMPS), L-NAME (3 mmol/L), GK activator (PKGa; 1 μmol/L 8-Bromo-cGMP), and L-arginine (L-Arg; 1 mmol/L) using the modified Boyden chamber assay. The migrated cells were counted and arbitrarily expressed relative to VEGF-migrated wild-type ECs (100%). $^{*}P<0.01$, $^{**}P<0.005$, $^{***}P<0.001$ vs VEGF-treated control cells (n=5). B, Tubular formation of ECs was assessed with or without L-NAME (3 mmol/L) or L-Arg (1 mmol/L). Arrows indicates tubular formation. Total vessel lengths in the microscopic fields were evaluated (n=4 each). $^{*}P<0.05$, $^{**}P<0.01$ vs VEGF-treated control cells. C, Histological appearance (hematoxylin-eosin staining) of the Matrigel plug sections showing EC-forming vessels (arrowheads). The vessels were counted (n=6). $^{*}P<0.01$.

more, treatment with L-NAME attenuated VEGF-mediated Rac1 activation in the wild-type ECs, whereas addition of L-arginine to the PYK2-deficient ECs restored the response, indicating that PYK2-mediated Rac1 activation is NO dependent (Figure 7B).

Taniyama et al[25] showed that in the angiotensin II–stimulated cells (vascular smooth muscle cells), Ca^{2+}-activated PYK2 acts as a scaffold for Src-dependent phosphorylation of 3-phosphoinositide-dependent protein kinase, the activator of Akt, whereas VEGF-induced Akt activation appears to be Ca^{2+} independent (Figure 3C). We therefore evaluated the target of PYK2 in the VEGF-mediated signaling pathways leading to Akt activation or Ca^{2+} mobilization. We found that VEGF stimulation causes PYK2 association with Src in the wild-type ECs, leading to the phosphorylation of Src (Figure 7C) and Akt (Figures 2B and 7C). PYK2 deficiency significantly inhibited VEGF-mediated Src and Akt activation, and inhibition of Src activity by PP1 blocked Akt and PYK2 phosphorylation (Figures 2B and 7C). Immunoprecipitation experiments indicated that Src, but not PYK2, is closely associated with the p85 subunit of PI3K and that the Src/PI3K complex binds to PYK2 in response to VEGF (Figure 7C, bottom).

To study PYK2-mediated Ca^{2+} signaling after stimulation with VEGF, we studied PLCγ1 activation, known to cause an increase in Ca^{2+} level.[26] We found that VEGF-mediated Src association with PLCγ1 and phosphorylation of ^{783}Tyr-PLCγ1 (both basal and VEGF induced) were significantly decreased in the PYK2-deficient cells and that the treatment with the Src inhibitor PP1 abolished VEGF-induced PLCγ1 phosphorylation (Figure 7D).

Taken together, it is likely that the direct target of PYK2 is Src and that Src-bound PI3-kinase and Src-bound PLCγ are involved in activation of Akt and Ca^{2+} mobilization, respectively.

Discussion

Tyrosine kinases have been assumed to be the upstream molecule for PI3K-Akt-eNOS or Ca^{2+}-eNOS pathways. eNOS is activated by Akt, and intracellular Ca^{2+} upregulates eNOS activity, raising the possibility that Ca^{2+}-dependent tyrosine kinase PYK2 is a possible eNOS activator. This study provides the first evidence that (1) PYK2 deficiency attenuates VEGF-mediated eNOS phosphorylation associated with decreased Akt activation and intracellular Ca^{2+} mobilization, (2) PYK2 is associated with the Src/PI3K complex and inhibition of Src blocked Akt phosphorylation, (3) Ach-mediated vasodilation of the aorta was diminished by decreased cGMP production in $PYK2^{-/-}$ mice, and (4) PYK2 plays a central role in VEGF- or ischemia-mediated eNOS activation followed by angiogenic response in which VEGF-induced EPC mobilization, VEGF-dependent migration, actin cytoskeletal reorganization associated with reduced Rac1 activation were markedly inhibited in the PYK2-deficient

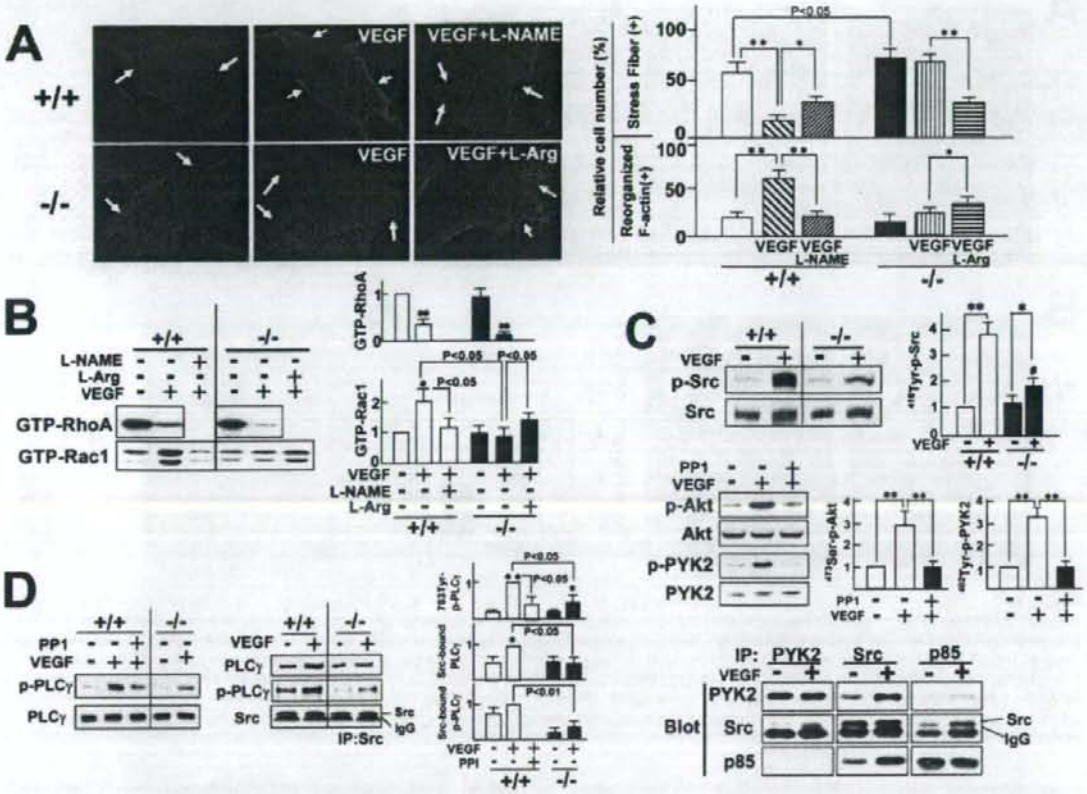

Figure 7. Impaired reorganization of F-actin in PYK2-deficient cells. A, F-actin structure of ECs. ECs were cultured on the fibronectin-coated glass chamber. After 16 hours of starvation (0.5% serum) with or without preincubation by L-arginine (1 mmol/L) or L-NAME (3 mmol/L), ECs were stimulated with VEGF (100 ng/mL) for 30 minutes, fixed with 4% paraformaldehyde, and permeabilized with 0.02% triton, and F-actin was stained with TRITC-labeled phalloidin. Representative staining was shown (n=7 each). Yellow arrows indicate the stress fiber; white arrows, accumulated F-actin at the plasma membrane. The cells with stress fiber or accumulated F-actin at the plasma membrane were counted, and the ratio (%) relative to total attaching cells was shown. *P<0.05, **P<0.01. B, Measurement of the VEGF-induced RhoA:GTP/Rac1:GTP. After 16 hours of starvation with or without L-NAME or L-arginine, ECs were incubated by VEGF for 5 minutes. Cell lysates were incubated with GST-RBD (Rho-binding domain) and GST-PBD (p21-binding domain) bound to glutathione beads as described in the Methods section of the online Data Supplement. The amount of RhoA:GTP and Rac1:GTP complex was determined by immunoblot with anti-RhoA and anti-Rac1 antibodies. *P<0.05, **P<0.01 (n=4 each) vs non-stimulated group. C, After 16 hours of starvation with or without PP1, ECs were incubated with VEGF for 5 minutes. Top, Cell lysates were subjected to Western blotting with antibodies against anti–^{416}Tyr-phosphorylated-Src or Src. Middle, Cell lysates of the wild-type ECs were analyzed by Western blotting with antibodies against Akt, ^{473}Ser-phosphorylated Akt, PYK2, and ^{402}Tyr-phosphorylated PYK2. Bottom, Cell lysates of the wild-type ECs were immunoprecipitated (IP), followed by Western blotting using antibodies against anti-PYK2, Src, and p85 subunit of PI3-kinase. *P<0.05, **P<0.005 (n=5 each experiment). D, After 16 hours of starvation with or without PP1, ECs were stimulated with VEGF for 5 minutes. Cell lysates were subjected to immunoblotting with antibodies against PLCγ1 or ^{783}Tyr-phosphorylated PLCγ1, plus immunoprecipitation with anti-Src antibody, followed by immunoblot with antibodies against PLCγ1, ^{783}Tyr-phosphorylated PLCγ1, or Src. *P<0.05, **P<0.005 (n=4 each) vs nonstimulated groups. #P<0.05 vs VEGF-stimulated wild-type ECs.

ECs. Cell migration reportedly requires the recycled mobilization of actin from the old focal adhesion toward the plasma membrane of the leading edge to form the lamellipodia and new focal contact,[27] suggesting that impaired reorganization of the F-actin at the plasma membrane plausibly causes attenuated migration of the PYK2-deficient ECs.

eNOS activation is dependent on an increase in $[Ca^{2+}]i$ and the binding of Ca^{2+}/calmodulin to the enzyme, leading to conformational change to displace the autoinhibitory loop.[28] If Ca^{2+} mobilization is totally abolished, administration of the eNOS substrate arginine could not restore eNOS activity. However, VEGF-induced increase in $[Ca^{2+}]i$ and subsequent translocation of NFATc2 in PYK2-deficient ECs remain ≈23% and ≈32%, respectively, of the wild-type cells (Figure 3). This increase in $[Ca^{2+}]i$ could cause the conformational change in eNOS, resulting in the recovery in eNOS activation after arginine administration.

The present study showed that PYK2 deficiency attenuates VEGF-mediated association of Src with PLCγ1 and phosphorylation of PLCγ1. VEGF was shown to stimulate the

association of VEGF receptor-2 with Src, and subsequent Src activation was a requisite for VEGF-mediated PLCγ1 activation.[29] Taken together, it is conceivable that the lack of intracellular Ca^{2+} mobilization in VEGF-stimulated PYK2-deficient cells is due to the inhibition of Src-associated PLCγ activation.

Src and PYK2 are mutually activated in a stepwise manner. Association of Src-SH2-domain with ^{402}Tyr-phosphorylated-PYK2 leads to conformational change in Src to release the internal autoinhibition, resulting in the upregulation of its activity. Conversely, activated Src phosphorylates ^{881}Tyr-PYK2, leading to the downstream Grb2/Ras/MAPK pathway.[10] In response to VEGF receptor-2 stimulation, Src binds toward the phosphorylated ^{1212}Tyr of VEGF receptor-2 with its SH2 domain, leading to Src activation.[30] In addition, VEGF promotes association of VEGF receptor-2 with integrin ($\alpha V\beta 3$) and transmits integrin-dependent cell biological responses.[31] Activation of integrin ($\alpha V\beta 3$) induces phosphorylation of ^{402}Tyr-PYK2 and its association with integrin $\beta 3$.[32] Integrin-activated PYK2 is associated with Src[33] and involved in VEGF-mediated cell migration.[34] Furthermore, integrin ($\alpha V\beta 5$) plays a crucial role in angiogenesis,[35] and inhibition of integrin ($\alpha V\beta 5$) disrupted VEGF-mediated and Src-dependent angiogenesis.[36] Thus, PYK2/Src complex is likely to integrate integrin with the VEGF receptor-2 signaling system.

Fluid shear stress–mediated activation of eNOS is dependent on Ca^{2+} mobilized through a mechanical stress–activated Ca^{2+} channel on the plasma membrane, whereas a Ca^{2+}-independent system has been reported recently. Fleming et al[37] demonstrated that shear stress elicits Src-mediated phosphorylation of platelet EC adhesion molecule-1 (PECAM-1) at the cell-to-cell contact, which is crucial for subsequent activation of Akt and eNOS. Furthermore, Tzima et al[38] showed that PECAM-1 forms a mechanosensory complex with VEGF receptor-2, leading to activation of PI3-kinase. These findings suggest that VEGF receptor-2 is involved in Src/PECAM-1–mediated Akt/eNOS activation in Ca^{2+}-independent manner. Unlike PECAM-1, PYK2 is localized at the cell-to–extracellular-matrix contact region.[8,33] VEGF promotes the association of VEGF receptor-2 with integrin and integrin-dependent cell biological responses.[31] Thus, the PYK2/Src complex transmits the VEGF signals in association with extracellular matrix/integrins, suggesting that the Ca^{2+}-independent Src/PECAM-1 system is unlikely to be involved in PYK2-mediated Src activation.

Because the blood flow recovery ratio in the ischemic limbs was increased ≈5-fold on day 7 compared with the day 0 control level (Figure 5A), hemodynamic shear stress also could be proportionally elevated in the newly formed vessels. Shear stress was shown to elicit the phosphorylation of ^{1177}Ser-eNOS by activating both Akt and PKA.[28] As shown in Figure 2A, Akt, AMPK, and PKA showed peak phosphorylation on day 1 and at 2 hours, respectively, and then PKA and AMPK reversed to the baseline level on day 7, whereas moderate activation of Akt was observed on day 7 (210% increase compared with the basal level), suggesting that Akt, rather than PKA and AMPK, is involved in the eNOS activation 7 days after limb ischemia. However, further studies are required to define the involvement of other kinases associated with flow shear stress.

Conclusions

This analysis of PYK2$^{-/-}$ mice demonstrates the critical role of PYK2 in Akt/NO signals activated by vasoactive substances or ischemic stress that modulates the vascular tonus or angiogenesis. These findings indicate that PYK2 can operate as a modulator for extracellular versatile stimuli, leading to eNOS activation, and is closely involved in the receptor- or ischemia-activated NO signaling events and thus regulates the cytoskeleton structure, vasoreactive function, or angiogenic response.

Acknowledgment

The authors profoundly appreciate Dr Nobuo Shirahashi for his advice and help with the statistical analysis.

Source of Funding

This work was supported by grants from the Ministry of Education, Culture, Sports, Science and Technology of Japan (grants 13670763 and 15590778 to Dr Okigaki).

Disclosures

None.

References

1. Shesely EG, Maeda N, Kim HS, Desai KM, Krege JH, Laubach VE, Sherman PA, Sessa WC, Smithies O. Elevated blood pressures in mice lacking endothelial nitric oxide synthase. *Proc Natl Acad Sci U S A*. 1996;93:13176–13181.
2. Fukumura D, Gohongi T, Kadambi A, Izumi Y, Ang J, Yun CO, Buerk DG, Huang PL, Jain RK. Predominant role of endothelial nitric oxide synthase in vascular endothelial growth factor-induced angiogenesis and vascular permeability. *Proc Natl Acad Sci U S A*. 2001;98:2604–2609.
3. Fulton D, Gratton JP, McCabe TJ, Fontana J, Fujio Y, Walsh K, Franke TF, Papapetropoulos A, Sessa WC. Regulation of endothelium-derived nitric oxide production by the protein kinase Akt. *Nature*. 1999;399:597–601.
4. Dimmeler S, Fleming I, Fisslthaler B, Hermann C, Busse R, Zeiher AM. Activation of nitric oxide synthase in endothelial cells by Akt-dependent phosphorylation. *Nature*. 1999;399:601–605.
5. Haynes MP, Li L, Sinha D, Russell KS, Hisamoto K, Baron R, Collinge M, Sessa WC, Bender Jr. Src kinase mediates phosphatidylinositol 3-kinase/Akt-dependent rapid endothelial nitric-oxide synthase activation by estrogen. *J Biol Chem*. 2003;278:2118–2123.
6. Lev, S. Moreno H, Martinez R, Canoll P, Peles E, Musacchio JM, Plowman GD, Rudy B, Schlessinger J. Protein tyrosine kinase PYK2 involved in Ca(2+)-induced regulation of ion channel and MAP kinase functions. *Nature*. 1995;376:737–745.
7. Yu H, Marchetto GS, Dy R, Hunter D, Calvo B, Dawson TL, Wilm M, Anderegg RJ, Graves LM, Earp HS. Activation of a novel calcium-dependent protein-tyrosine kinase: correlation with c-Jun N-terminal kinase but not mitogen-activated protein kinase activation. *J Biol Chem*. 1996;271:29993–29998.
8. Astier A, Avraham H, Manie SN, Groopman J, Canty T, Avraham S, Freedman AS. The related adhesion focal tyrosine kinase is tyrosine-phosphorylated after beta1-integrin stimulation in B cells and binds to p^{130cas}. *J Biol Chem*. 1997;272:228–232.
9. Tian D, Litvak V, Lev S. Cerebral ischemia and seizures induce tyrosine phosphorylation of PYK2 in neurons and microglial cells. *J Neurosci*. 2000;20:6478–6487.
10. Dikic I, Tokiwa G, Lev S, Courtneidge SA, Schlessinger J. A role for Pyk2 and Src in linking G-protein-coupled receptors with MAP kinase activation. *Nature*. 1996;383:547–550.
11. Okigaki M, Davis C, Falasca M, Harroch S, Felsenfeld D, Sheetz MP, Schlessinger J. Pyk2 regulates multiple signaling events crucial for macrophage morphology and migration. *Proc Natl Acad Sci U S A*. 2003;100:10740–10745.

12. Tamarat R, Silvestre JS, Kubis N, Benessiano J, Duriez M, deGasparo M, Henrion D, Levy BI. Endothelial nitric oxide synthase lies downstream from angiotensin II-induced angiogenesis in ischemic hindlimb. *Hypertension*. 2002;39:830–835.
13. Michell BJ, Chen Z, Tiganis T, Stapleton D, Katsis F, Power DA, Sim AT, Kemp BE. Coordinated control of endothelial nitric-oxide synthase phosphorylation by protein kinase C and the cAMP-dependent protein kinase. *J Biol Chem*. 2001;276:17625–17628.
14. Boo YC, Sorescu G, Boyd N, Shiojima I, Walsh K, Du J, Jo H. Shear stress stimulates phosphorylation of endothelial nitric-oxide synthase at Ser1179 by Akt-independent mechanisms: role of protein kinase A. *J Biol Chem*. 2002;277:3388–3396.
15. Yamamoto K, Sokabe T, Matsumoto T, Yoshimura K, Shibata M, Ohura N, Fukuda T, Sato T, Sekine K, Kato S, Isshiki M, Fujita T, Kobayashi M, Kawamura K, Masuda H, Kamiya A, Ando J. Impaired flow-dependent control of vascular tone and remodeling in P2X4-deficient mice. *Nat Med*. 2006;12:133–137.
16. Hernandez GL, Volpert OV, Iniguez MA, Lorenzo E, Martinez-Martinez S, Grau R, Fresno M, Redondo JM. Selective inhibition of vascular endothelial growth factor-mediated angiogenesis by cyclosporin A: roles of the nuclear factor of activated T cells and cyclooxygenase 2. *J Exp Med*. 2001;193:607–620.
17. Murohara T, Asahara T, Silver M, Bauters C, Masuda H, Kalka C, Kearney M, Chen D, Symes JF, Fishman MC, Huang PL, Isner JM. Nitric oxide synthase modulates angiogenesis in response to tissue ischemia. *J Clin Invest*. 1998;101:2567–2578.
18. Aicher A, Heeschen C, Mildner-Rihm C, Urbich C, Ihling C, Technau-Ihling K, Zeiher AM, Dimmeler S. Essential role of endothelial nitric oxide synthase for mobilization of stem and progenitor cells. *Nat Med*. 2003;9:1370–1376.
19. Smolenski A, Poller W, Walter U, Lohmann SM. Regulation of human endothelial cell focal adhesion sites and migration by cGMP-dependent protein kinase I. *J Biol Chem*. 2000;275:25723–25732.
20. Surks HK, Mochizuki N, Kasai Y, Georgescu SP, Tang KM, Ito M, Lincoln TM, Mendelsohn ME. Regulation of myosin phosphatase by a specific interaction with cGMP- dependent protein kinase Ialpha. *Science*. 1999;286:1583–1587.
21. Ren XD, Kiosses WB, Schwartz MA. Regulation of the small GTP-binding protein Rho by cell adhesion and the cytoskeleton. *EMBO J*. 1999;18:578–585.
22. Benard V, Bohl BP, Bokoch GM. Characterization of Rac and Cdc42 activation in chemoattractant-stimulated human neutrophils using a novel assay for active GTPases. *J Biol Chem*. 1999;274:13198–13204.
23. Ridley AJ, Hall A. The small GTP-binding protein rho regulates the assembly of focal adhesions and actin stress fibers in response to growth factors. *Cell*. 1992;70:389–399.
24. Tokiwa G, Dikic I, Lev S, Schlessinger J. Activation of Pyk2 by stress signals and coupling with JNK signaling pathway. *Science*. 1996;273:792–794.
25. Taniyama Y, Weber DS, Rocic P, Hilenski L, Akers ML, Park J, Hemmings BA, Alexander RW, Griendling KK. Pyk2- and Src-dependent tyrosine phosphorylation of PDK1 regulates focal adhesions. *Mol Cell Biol*. 2003;23:8019–8029.
26. Carroll DJ, Ramarao CS, Mehlmann LM, Roche S, Terasaki M, Jaffe LA. Calcium release at fertilization in starfish eggs is mediated by phospholipase Cgamma. *J Cell Biol*. 1997;138:1303–1311.
27. Lawson MA, Maxfield FR. Ca^{2+}- and calcineurin-dependent recycling of an integrin to the front of migrating neutrophils. *Nature*. 1995;377:75–79.
28. Fleming I, Busse R. Molecular mechanisms involved in the regulation of the endothelial nitric oxide synthase. *Am J Physiol Regul Integr Comp Physiol*. 2003;284:R1–R12.
29. He H, Venema VJ, Gu X, Venema RC, Marrero MB, Caldwell RB. Vascular endothelial growth factor signals endothelial cell production of nitric oxide and prostacyclin through flk-1/KDR activation of c-Src. *J Biol Chem*. 1999;274:25130–25135.
30. Meyer RD, Dayanir V, Majnoun F, Rahimi N. The presence of a single tyrosine residue at the carboxyl domain of vascular endothelial growth factor receptor-2/FLK-1 regulates its autophosphorylation and activation of signaling molecules. *J Biol Chem*. 2002;277:27081–27087.
31. Soldi R, Mitola S, Strasly M, Defilippi P, Tarone G, Bussolino F. Role of alphavbeta3 integrin in the activation of vascular endothelial growth factor receptor-2. *EMBO J*. 1999;18:882–892.
32. Butler B, Blystone SD. Tyrosine phosphorylation of beta3 integrin provides a binding site for Pyk2. *J Biol Chem*. 2005;280:14556–14562.
33. Duong LT, Lakkakorpi PT, Nakamura I, Machwate M, Nagy RM, Rodan GA. PYK2 in osteoclasts is an adhesion kinase, localized in the sealing zone, activated by ligation of alpha (v) beta3 integrin, and phosphorylated by src kinase. *J Clin Invest*. 1998;102:881–892.
34. Avraham HK, Lee TH, Koh Y, Kim TA, Jiang S, Sussman M, Samarel AM, Avraham S. Vascular endothelial growth factor regulates focal adhesion assembly in human brain microvascular endothelial cells through activation of the focal adhesion kinase and related adhesion focal tyrosine kinase. *J Biol Chem*. 2003;278:36661–36668.
35. Friedlander M, Brooks PC, Shaffer RW, Kincaid CM, Varner JA, Cheresh DA. Definition of two angiogenic pathways by distinct alpha v integrins. *Science*. 1995;270:1500–1502.
36. Hood JD, Frausto R, Kiosses WB, Schwartz MA, Cheresh DA. Differential alphav integrin-mediated Ras-ERK signaling during two pathways of angiogenesis. *J Cell Biol*. 2003;162:933–943.
37. Fleming I, Fisslthaler B, Dixit M, Busse R. Role of PECAM-1 in the shear-stress-induced activation of Akt and the endothelial nitric oxide synthase (eNOS) in endothelial cells. *J Cell Sci*. 2005;118:4103–4111.
38. Tzima E, Irani-Tehrani M, Kiosses WB, Dejana E, Schultz DA, Engelhardt B, Cao G, DeLisser H, Schwartz MA. A mechanosensory complex that mediates the endothelial cell response to fluid shear stress. *Nature*. 2005;437:426–431.

CLINICAL PERSPECTIVE

Although endothelial dysfunction causes atherosclerosis or vascular aging, drugs to improve endothelial functions have not been developed. Nitric oxide (NO) plays pivotal roles in the maintenance of endothelial function and vascular homeostasis, including vasodilatation, antiinflammatory effect, anticoagulation, antiproliferative effect of vascular smooth muscle cells, angiogenesis, and vasculogenesis. NO is produced by endothelial NO synthase (eNOS); therefore, a drug that upregulates eNOS function may improve endothelial function. For this purpose, it is important to clarify the molecular mechanism to activate eNOS. In the present study, we showed that tyrosine kinase PYK2 plays a crucial role in eNOS activation. Both PYK2 and eNOS are activated by hemodynamic mechanical stress, ischemic stress, and stimulation with endothelial growth factors, and PYK2 transmits calcium and Akt signaling pathways, both of which activate eNOS, suggesting that the drug developed to activate PYK2 may be feasible therapy for maintaining vascular homeostasis in various stress conditions. However, PYK2 also is involved in angiotensin II–mediated signaling to induce atherosclerosis, including vasoconstriction, vascular inflammation, and proliferation of vascular smooth muscle cells, indicating that PYK2 has dual effects on vascular function. The role of PYK2 in the maintenance of vascular homeostasis should be investigated further.

Circulation Research

JOURNAL OF THE AMERICAN HEART ASSOCIATION

American Heart Association.

Learn and Live.

New Targeted Angiogenic Strategy: Bursting Bubbles

Tomosaburo Takahashi and Hiroaki Matsubara

Circ. Res. 2007;101;232-233
DOI: 10.1161/CIRCRESAHA.107.158253
Circulation Research is published by the American Heart Association. 7272 Greenville Avenue, Dallas, TX 72514
 Print ISSN: 0009-7330. Online ISSN: 1524-4571

See related article, pages 295–303

New Targeted Angiogenic Strategy
Bursting Bubbles

Tomosaburo Takahashi, Hiroaki Matsubara

Although recent procedural advances in revascularization such as percutaneous coronary intervention and coronary artery bypass grafting improve quality of life and prognosis of the patients with ischemic diseases, these is still a subset of patients who are refractory to these conventional therapies and have poor prognosis. Therapeutic angiogenesis might offer a novel approach to these patients. Therapeutic angiogenesis involves an intervention to induce the formation of new blood vessels to restore the arterial blood and oxygen supply to ischemic tissues.[1] Here, the term "angiogenesis" represents the process of new blood vessel formation in general (although the same term is also used to describe a more specific biological process in which the new capillaries sprout from preexisting vessels).

Evolving knowledge of mechanisms of new blood vessel formation has raised the expectations for therapeutic angiogenesis as a treatment option. Recent studies have identified many angiogenic growth factors, vascular transcription factors, and the cells involved in neovascularization.[1,2] Current potential strategies for therapeutic angiogenesis include delivering an angiogenic factor as a protein or a gene, and supplying cells which themselves are vascular progenitors or are releasing angiogenic factors. These strategies have worked in animal studies and in initial small scale open-labeled clinical trials. However, in larger, double-blinded controlled trials, therapeutic angiogenesis approaches have failed to show clinical benefits.[1,2] Why? Perhaps there are subtle differences in angiogenesis between animals and humans, or the ischemic pathophysiology of animal models and human diseases are dissimilar. Another possibility is technical difficulties in translating the biology into the practice.

In this issue of *Circulation Research*, Leon-Poi and colleagues report that targeted delivery of vascular endothelial growth factor (VEGF) gene using ultrasound-mediated destruction of cationic lipid microbubbles restores microvascular blood flow in a rat model of chronic hindlimb ischemia.[3] Ultrasound-targeted microbubble destruction uses ultrasound contrast agents, mostly perfluorocarbon bubbles stabilized with albumin or a lipid shell. When insonified at high acoustic power, these agents oscillate, resulting in microbubble disintegration.[4,5] This microbubble destruction has been shown to induce biophysical effects in the vicinity of contrast agents, and the therapeutic use of this phenomenon has been proposed for delivery of genes or drugs, and direct mechanical effects. One of the advantages of this method is that these bubbles cross the pulmonary circulation, so that the agents can be administrated intravenously, and reach any part of the body with arterial blood supply. And, at the desired sites, the agents can be activated or delivered by ultrasound. Leon-Poi et al coated the microbubbles with VEGF-expressing plasmid, intravenously administrated these bubbles, and then transferred the gene at the site of ischemia with ultrasound in hindlimb ischemia model.[3] This model of ischemia is chronic, because the gene was transferred 14 days after common iliac artery ligation.

Leon-Poi et al observed a significant increase in tissue perfusion mainly through the process of arteriogenesis, rather than angiogenesis in a narrow sense.[3] Arteriogenesis refers to the maturation or de novo synthesis of collateral vessels. The effect of VEGF gene transfer with this method on arteriogenesis rather than angiogenesis is intriguing, as remodeling or development of collaterals could be much more effective than an increase in capillary bed to restore the blood flow in the setting of flow-limiting proximal conduit artery lesions. It will be an important issue to determine whether the preferential effect on arteriogenesis is associated with the method of gene delivery, ultrasonic destruction of microbubble destruction (Figure).

Although the gene delivery is an important application of ultrasound-mediated microbubble destruction,[4–6] use of this method is not limited to gene therapy. Acoustic cavitation leads to microbubble oscillation and collapse. Electron microscopic analysis showed transient pore formation on cell membrane immediately after microbubble destruction, called sonoporation.[4,5] These mechanical effects facilitate entry of gene into the cells. At the same time, these mechanical forces affect nearby cells and tissues in vicinity of microbubble destruction. For example, microbubble destruction can facilitate thrombolysis in combination with thrombolytic agents such as urokinase and tissue plasminogen activator.[7,8] Furthermore, ultrasound-mediated microbubble destruction itself can be angiogenic, as ultrasound-mediated microbubble destruction has been shown to be able to induce capillary rupture and increase the density of arterioles in ischemic muscle with local recruitment of VEGF producing inflammatory cells.[9,10] Although capillary rupture with higher energies of ultrasound is just a step from adverse tissue damage, even with ultrasound without capillary rupture, ultrasound-mediated microbubble destruction has direct effects on vasculature and surrounding tissues. These effects can be

From the Department of Cardiovascular Medicine (T.T., H.M.), Kyoto Prefectural University of Medicine, Kyoto, Japan; Department of Experimental Therapeutics (T.T., H.M.), Translational Research Center, Kyoto University Hospital, Kyoto, Japan.

Correspondence to Tomosaburo Takahashi, Department of Cardiovascular Medicine, Kyoto Prefectural University of Medicine, 465 Kajii-cho Kawaramachi-Hirokoji, Kamigyo-ku, Kyoto 602-8566, Japan. E-mail ttaka@koto.kpu-m.ac.jp

(*Circ Res.* 2007;101:232-233.)

***Circulation Research* is available at http://circres.ahajournals.org**
DOI: 10.1161/CIRCRESAHA.107.158253

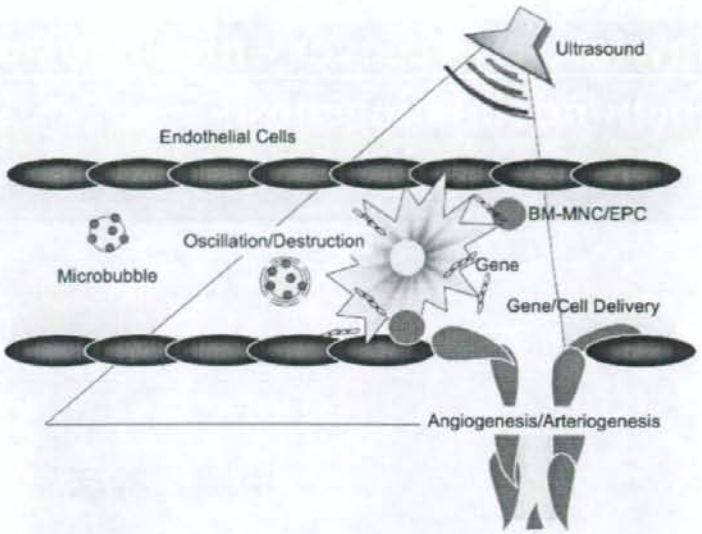

Schematic diagram of ultrasound-mediated microbubble destruction. Microbubbles enclosing therapeutic agents such as genes or drugs reach the local sites through circulation. At the desired site, ultrasound is applied, which oscillates and collapses the microbubbles, leading to direct biophysical effects on tissue or the delivery of therapeutic agents.

used for potential therapies, especially when combined with other modalities. One such example is microbubble destruction in combination with cell therapy. We have shown that targeted delivery of bone marrow-derived mononuclear cells by ultrasound-mediated microbubble destruction significantly enhances angiogenic response both in an ischemic hindlimb model and in a δ-sarcoglycan deficient cardiomyopathy model.[11,12] In the ischemic hindlimb model, ultrasound-mediated microbubble destruction induces platelet activation on the surface of endothelium, and subsequent induction of adhesion molecules on endothelium, which in turn stimulates recruitment of angiogenic mononuclear cells and enhances new vessel formation.[11] Ultrasound-mediated targeted cardiac delivery of marrow-derived mononuclear cells also efficiently enhances regional blood flow in myopathic hamsters, leading to improvement of cardiac function.[12]

Recent proof-of-principal studies show that ultrasound-mediated microbubble destruction has great potential to target various substrates including genes, proteins, drugs and cells to the desired sites. However, before this strategy is adopted in the clinic, many issues have to be resolved. Which patients are ideal subjects? What tissues are ideal target locations? What proteins and cells are ideal substrates to be delivered by microbubbles? Furthermore, technical issues of ultrasound-mediated microbubble destruction such as microbubble composition and ultrasound application must be refined. More collaboration between clinicians, biologist, chemists and engineers is needed to bring this exciting technique into the clinic.

Sources of Funding

This work was supported by Grants-in-Aid from the Ministry of Education, Culture, Sports, Science and Technology of Japan, and Grants-in-Aid from the Ministry of Health, Labor, and Welfare of Japan.

Disclosures

None.

References

1. Simons M. Angiogenesis: where do we stand now? *Circulation.* 2005; 111:1556–1566.
2. Shantsila E, Watson T, Lip GY. Endothelial progenitor cells in cardiovascular disorders. *J Am Coll Cardiol.* 2007;49:741–752.
3. Leong-Poi H, Kuliszewski MA, Lekas M, Sibbald M, Teichert-Kuliszewska K, Klibanov AL, Stewart DJ, Lindner JR. Therapeutic Arteriogenesis by Ultrasound-Mediated Vegf165 Plasmid Gene Delivery to Chronically Ischemic Skeletal Muscle. *Circ Res.* 2007;101:295–303.
4. Bekeredjian R, Grayburn PA, Shohet RV. Use of ultrasound contrast agents for gene or drug delivery in cardiovascular medicine. *J Am Coll Cardiol.* 2005;45:329–335.
5. Newman CM, Bettinger T. Gene therapy progress and prospects: ultrasound for gene transfer. *Gene Ther.* 2007;14:465–475.
6. Kondo I, Ohmori K, Oshita A, Takeuchi H, Fuke S, Shinomiya K, Noma T, Namba T, Kohno M. Treatment of acute myocardial infarction by hepatocyte growth factor gene transfer: the first demonstration of myocardial transfer of a "functional" gene using ultrasonic microbubble destruction. *J Am Coll Cardiol.* 2004;44:644–653.
7. Mizushige K, Kondo I, Ohmori K, Hirao K, Matsuo H. Enhancement of ultrasound-accelerated thrombolysis by echo contrast agents: dependence on microbubble structure. *Ultrasound Med Biol.* 1999;25:1431–1437.
8. Tachibana K, Tachibana S. Albumin microbubble echo-contrast material as an enhancer for ultrasound accelerated thrombolysis. *Circulation.* 1995;92:1148–1150.
9. Song J, Qi M, Kaul S, Price RJ. Stimulation of arteriogenesis in skeletal muscle by microbubble destruction with ultrasound. *Circulation.* 2002; 106:1550–1555.
10. Yoshida J, Ohmori K, Takeuchi H, Shinomiya K, Namba T, Kondo I, Kiyomoto H, Kohno M. Treatment of ischemic limbs based on local recruitment of vascular endothelial growth factor-producing inflammatory cells with ultrasonic microbubble destruction. *J Am Coll Cardiol.* 2005;46:899–905.
11. Imada T, Tatsumi T, Mori Y, Nishiue T, Yoshida M, Masaki H, Okigaki M, Kojima H, Nozawa Y, Nishiwaki Y, Nitta N, Iwasaka T, Matsubara H. Targeted delivery of bone marrow mononuclear cells by ultrasound destruction of microbubbles induces both angiogenesis and arteriogenesis response. *Arterioscler Thromb Vasc Biol.* 2005;25:2128–2134.
12. Zen K, Okigaki M, Hosokawa Y, Adachi Y, Nozawa Y, Takamiya M, Tatsumi T, Urao N, Tateishi K, Takahashi T, Matsubara H. Myocardium-targeted delivery of endothelial progenitor cells by ultrasound-mediated microbubble destruction improves cardiac function via an angiogenic response. *J Mol Cell Cardiol.* 2006;40:799–809.

KEY WORDS: therapeutic angiogenesis ■ gene therapy ■ ultrasound ■ microbubbles

Cardiac autophagy for self-recovery mechanism and mitochondrial biogenesis in adrenergic stress loaded failing heart

中岡　幹彦

Autophagyとは

—auto"自己" phagy"食べる"—

- 生体の恒常性を保つためのメカニズム
- 不要となった細胞質の蛋白やRNAなどを分解し、消化して再利用する
- 酵母から真核生物まで高度に保存されている

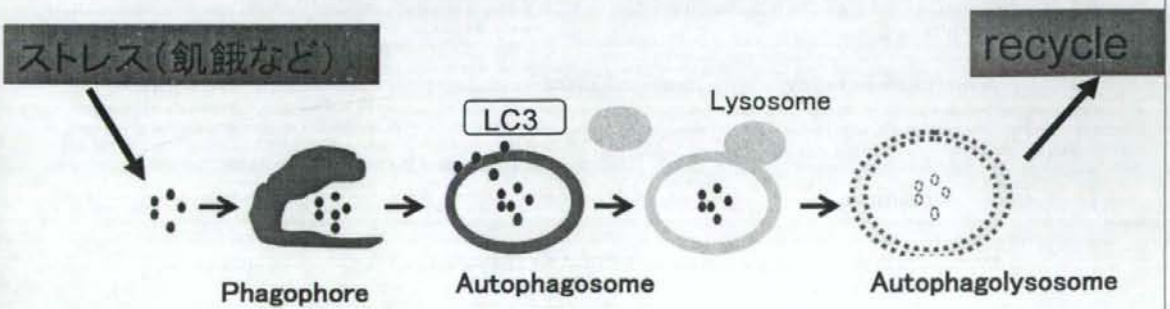

Autophagic Flux

Background2

Autophagy occurs in human failing heart

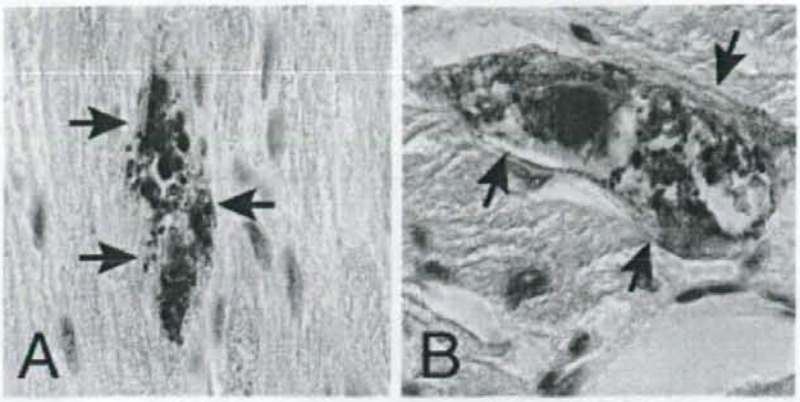

M.W.M. Knaapen et al. / Cardiovascular Research 51 (2001) 304 –312.

Nishida K. /Otsu K. / Circulation Journal 2008 September 5

Rothermel BA, Hill JA./ Autophagy 2007 ;3:632-4

Background3

However, pathological role of autophagy is unknown

Autophagy in the heart

・Autophagy in ischemic heart disease.	Gustafsson AB, Gottlieb RA. Circ Res. 2009 Jan 30;104(2):150-8. Review.
・Autophagy in load-induced heart disease.	Rothermel BA, Hill JA. Circ Res. 2008 Dec 5;103(12):1363-9. Review.
・The role of autophagy in the heart.	Nishida K, Kyoi S, Yamaguchi O, Sadoshima J, Otsu K. Cell Death Differ. 2009 Jan;16(1):31-8. Epub 2008 Nov 14. Review.

Background4

Adrenergic signaling pathways in cardiac myocytes

Several kinds of neurohormonal factors are activated
In heart failure

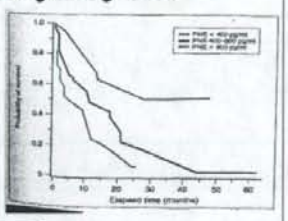

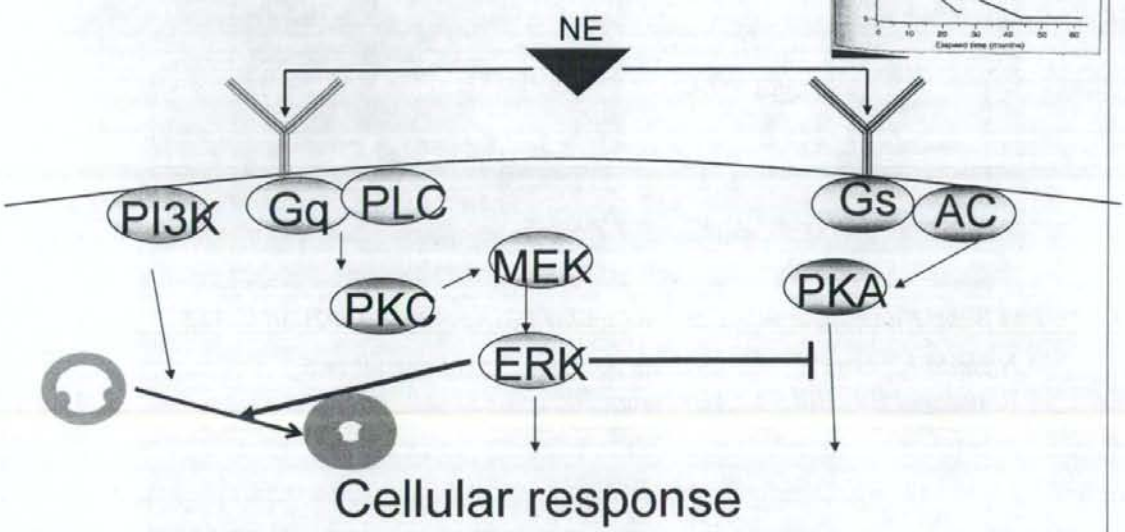

The initial purpose of the work

To test whether adrenergic stress stimulates autophagy in cardiac myocytes.

① 心筋におけるautophagyの評価方法を検討確認

② ①を用いて、交感神経のα-adrenergic receptor(AR)経路、β-adrenergic receptor(AR)経路,それぞれがautophagyに与える影響を検討。

③ 心筋autophagyが細胞の生死に与える影響を確認。

Method

In vitro

cardiac myocytes

Transfection
with GFP-tagged LC3

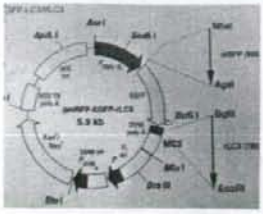

Adrenagic receptor(β , α)stimulation

- 3MA, Aspirin
- Monodansylcadaverine (MDC)

Quantification of autophagic flux & apoptosis

- Widefield fluorescence microscopy
- TUNEL staining
- MDC fluorescence
- Western blot(LC-3, Caspase3)

Result①Oxidative stress increased the accumulation of autophagosomes in cardiac myocytes

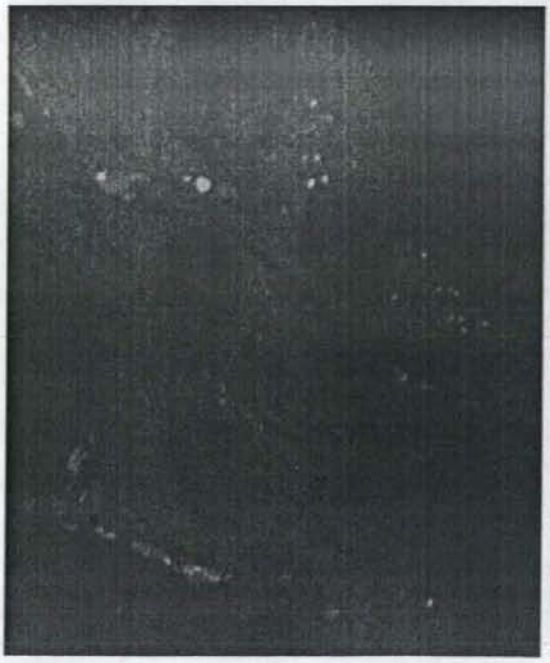

Control

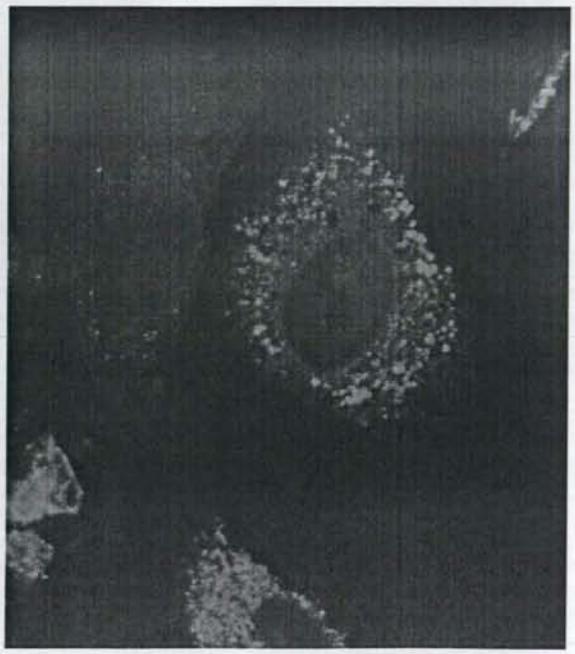

H_2O_2 10^{-6}M,2hr

Circulation Research

JOURNAL OF THE AMERICAN HEART ASSOCIATION

American Heart Association.
Learn and Live.

Stage-Specific Role of Endogenous Smad2 Activation in Cardiomyogenesis of Embryonic Stem Cells

Ryoji Kitamura, Tomosaburo Takahashi, Norio Nakajima, Koji Isodono, Satoshi Asada, Hikaru Ueno, Tomomi Ueyama, Toshikazu Yoshikawa, Hiroaki Matsubara and Hidemasa Oh

Circ. Res. 2007;101;78-87; originally published online May 31, 2007;
DOI: 10.1161/CIRCRESAHA.106.147264
Circulation Research is published by the American Heart Association. 7272 Greenville Avenue, Dallas, TX 72514
 Print ISSN: 0009-7330. Online ISSN: 1524-4571

Stage-Specific Role of Endogenous Smad2 Activation in Cardiomyogenesis of Embryonic Stem Cells

Ryoji Kitamura, Tomosaburo Takahashi, Norio Nakajima, Koji Isodono, Satoshi Asada, Hikaru Ueno, Tomomi Ueyama, Toshikazu Yoshikawa, Hiroaki Matsubara, Hidemasa Oh

Abstract—The role of Smads and their specific ligands during cardiomyogenesis in ES cells was examined. Smad2 was activated bimodally in the early and late phases of cardiac differentiation, whereas Smad1 was activated after the middle phase. Nodal and Cripto were expressed in the early stage and then downregulated, whereas transforming growth factor-β and activin were expressed only in the late phase. Suppression of early Smad2 activation by SB-431542 produced complete inhibition of endodermal and mesodermal induction but augmented neuroectodermal differentiation, followed by poor cardiomyogenesis, whereas inhibition during the late phase alone promoted cardiomyogenesis. Inhibitory effect of Smad2 on cardiomyogenesis in the late phase was mainly mediated by transforming growth factor-β, and inhibition of transforming growth factor-β–mediated Smad2 activation resulted in a greater replicative potential in differentiated cardiac myocytes and enhanced differentiation of nonmyocytes into cardiac myocytes. Thus, endogenous Smad2 activation is indispensable for endodermal and mesodermal induction in the early phase. In the late phase, endogenous transforming growth factor-β negatively regulates cardiomyogenesis through Smad2 activation by modulating proliferation and differentiation of cardiac myocytes. (***Circ Res.*** **2007;101:78-87.)**

Key Words: embryonic stem cells ■ cardiomyogenesis ■ Smad2 ■ TGF-β ■ differentiation

Embryonic stem (ES) cells are well-established pluripotent stem cells and capable of self-renewal and differentiation into derivatives of all 3 primary germ layers. With appropriate culture conditions, ES cells can differentiate into specialized cells including cardiac myocytes in vitro. The in vitro differentiation of ES cells into cardiac myocytes not only provides unique opportunities to study development of cardiac myocytes but also proposes the potential use of ES cell–derived cardiac myocytes for many medical applications such as cell transplantation therapy against various heart diseases and pharmacological testing on cardiac myocytes.[1] However, the molecular mechanisms governing differentiation of ES cells into specific lineages are poorly understood, and their comprehension would improve the efficiency of differentiation into specific cell types.

Members of transforming growth factor (TGF)-β superfamily are pleiotropic cytokines involved in many biological processes and signaling via heteromeric complexes of type I and type II serine/threonine kinase receptors.[2] On ligand binding and heterodimerization, the constitutively active type II receptor kinase phosphorylates the type I receptor, which in turn activates downstream signal transduction cascades including Smad pathways. According to the usage of different sets of type I receptors and receptor-regulated Smad (R-Smad), the superfamily members can be classified into 2 major branches: (1) the TGF-β/activin/Nodal branch and (2) the bone morphogenetic protein (BMP)/growth and differentiation factor (GDF) branch.[2] The TGF-β/activin/Nodal branch activates activin receptor–like kinase (ALK)-4, -5, and -7, which phosphorylate Smad2 and -3, whereas Smad1, -5, and -8 are substrates for the BMP/GDF branch through ALK-1, -2, -3, and -6.[2,3] The role of Smad1/5/8-activating BMP in cardiogenesis is relatively well documented. In chick embryo, BMP2 is able to induce expression of myocardial lineage markers in ectopic locations in vivo, and anterior lateral mesoderm explant cultures in vitro,[4] and Noggin, one of soluble BMP antagonists, prevents myocardial differentiation of lateral mesendoderm culture in vitro.[4] The dependence of myocardial specification on BMP signaling is evolutionally conserved, although several members of BMP have overlapping function in murine cardiac differentiation.[5] In murine teratocarcinoma P19CL6 cells, myocardial differentiation is shown to depend on functional BMP signals,[6] supporting the essential role for BMP signaling in cardiac specification. However, little is yet known about the function of Samd2/3-activating TGF-β, activin, and Nodal in cardiac differentiation.

Original received December 21, 2006; revision received May 16, 2007; accepted May 18, 2007.

From the Department of Cardiovascular Medicine (R.K., T.T., N.N, K.I., S.A., H.M.) and Department of Inflammation and Immunology (T.Y.), Kyoto Prefectural University of Medicine; Department of Experimental Therapeutics (R.K., T.T., N.N, K.I., S.A., T.U., H.M., H.O.), Translational Research Center, Kyoto University Hospital; and Department of Biochemistry and Molecular Pathophysiology (H.U.), University of Occupational and Environmental Health School of Medicine, Kitakyushu, Japan.

Correspondence to Tomosaburo Takahashi, Department of Cardiovascular Medicine, Kyoto Prefectural University of Medicine, 465 Kajii-cho Kawaramachi-Hirokoji, Kamigyo-ku, Kyoto 602-8566, Japan. E-mail ttaka@koto.kpu-m.ac.jp

Circulation Research **is available at http://circres.ahajournals.org** **DOI: 10.1161/CIRCRESAHA.106.147264**

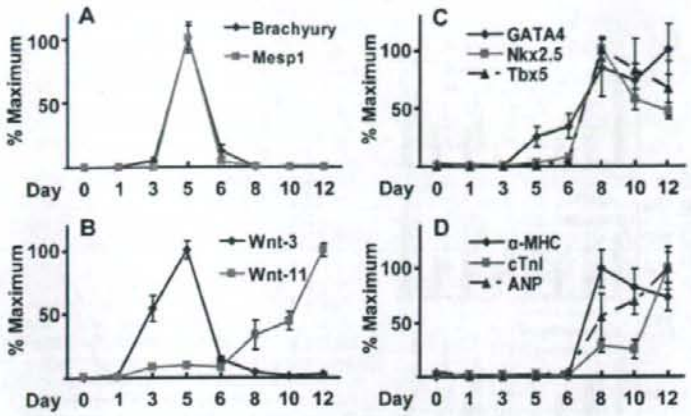

Figure 1. Cardiac differentiation programs in ES cells. ES cells were cultured in hanging drop suspension cultures for 5 days and then on gelatin-coated dishes for 7 more days. Cells were harvested at the indicated time points. Gene expression was analyzed by real-time kinetic PCR (A through D). A, Brachyury, Mesp1. B, Wnt-3, Wnt-11. C, GATA4, Nkx2.5, Tbx5. D, α-MHC, cTnI, ANP. The results were expressed relative to the level of 18S ribosomal RNA and plotted as percentages of the maximum.

In the present study, we hypothesized that Smad2 activation is involved in cardiomyogenesis and analyzed the roles of Smad2 and its specific ligands during in vitro differentiation of ES cells into cardiac myocytes.

Materials and Methods

An expanded Materials and Methods section can be found in the online supplement at http://circres.ahajournals.org.

ES Cell Culture and Differentiation

CGR8 mouse ES cells and ES cells stably transfected with α-myosin heavy chain (MHC) promoter-driven enhanced green fluorescent protein (EGFP) were used, and differentiation was induced by forming embryoid bodies (EBs) in the hanging drop suspension culture.[7]

Replication-Defective Recombinant Adenoviruses

Adenoviral vectors expressing a soluble type II TGF-β receptor (sTGF-β IIR), dominant negative mutant of Smad2 (Smad2 DN), or β-galactosidase (LacZ) were prepared as described.[8,9]

Flow Cytometric Analysis and Cell Sorting

α-MHC–EGFP ES cells were analyzed with a FACSCalibur Flow Cytometer or sorted with FACSAria cell sorter.

Immunostaining

Cells were stained with the primary antibody against sarcomeric α-actinin or βIII-tubulin (Sigma). Sorted cells were centrifuged onto polylysine slides and stained with anti–phospho-histone H3 antibody (Millipore).

5-Bromodeoxyuridine Incorporation Assay

Cells were labeled with 5-bromodeoxyuridine (BrdUrd) for 2 hours at day 8. Sorted cells were stained with anti-BrdUrd antibody (Roche).

Results

Cardiac Differentiation Programs in ES Cells

In vitro differentiation of ES cells was induced by forming cellular aggregates called EBs through the hanging drop method,[7] and spontaneously contracting cell clusters developed within EB outgrowths at day 7 (attached culture for 2 days after 5 days of hanging drop suspension culture). Early mesodermal markers, Brachyury and Mesp1, were transiently expressed around day 5 (Figure 1A). Wnt-3 expression was upregulated transiently between day 3 and 5, and Wnt-11 expression was upregulated with the differentiation (Figure 1B). Among the transcription factors crucial for cardiac differentiation, GATA4 expression was first detected at day 5, followed by expression of Nkx2.5 and Tbx5 (Figure 1C). The genes for myocardial structural proteins α-MHC and cardiac troponin (cTn)I and a cardiac-specific peptide, atrial natriuretic peptide (ANP), were expressed after day 8 (Figure 1D). These results were consistent with the previous reports[1,10] and indicated that the in vitro differentiation of ES cells recapitulates the developmental program of cardiac myocytes and that during the formation of EB in suspension culture, mesodermal induction occurs, and, thereafter, the specification and maturation of cardiac myocytes are executed.

Smad2 Shows Bimodal Activation in the Early and Late Phases, Which Is Mediated by Nodal/Cripto and TGF-β/Activin, Respectively

To assess how Smads were regulated during ES cell differentiation, expression and phosphorylation of Smad proteins were examined by immunoblot analysis with total and phospho-specific antibodies against Smads (Figure 2A and 2B). In undifferentiated ES cells, although both Smad1 and Smad2 were expressed, only Smad2 was robustly phosphorylated. Phosphorylation of Smad1 was detected at day 5, which remained detectable thereafter. In marked contrast, Smad2 phosphorylation was decreased on induction of differentiation and disappeared at day 5. Phosphorylated Smad2 was detected again at day 8 and remained detectable until day 12. The expression of Smad2 was also regulated during ES cell differentiation. The expression of Smad2 was decreased during the initial phase and increased again in the late phase (Figure 2A and 2B), whereas the biphasic activation of Smad2 was still evident even after normalized with the expression of Smad2 (Figure 2B). These results indicated that Smad1 and Smad2 are differently regulated and that Smad2 shows unique bimodal activation in ES cell differentiation. As Smad1 activation has been shown to be involved in cardiomyogenesis, we focused on the role of Smad2 activation in cardiomyogenesis. We, therefore, analyzed the gene

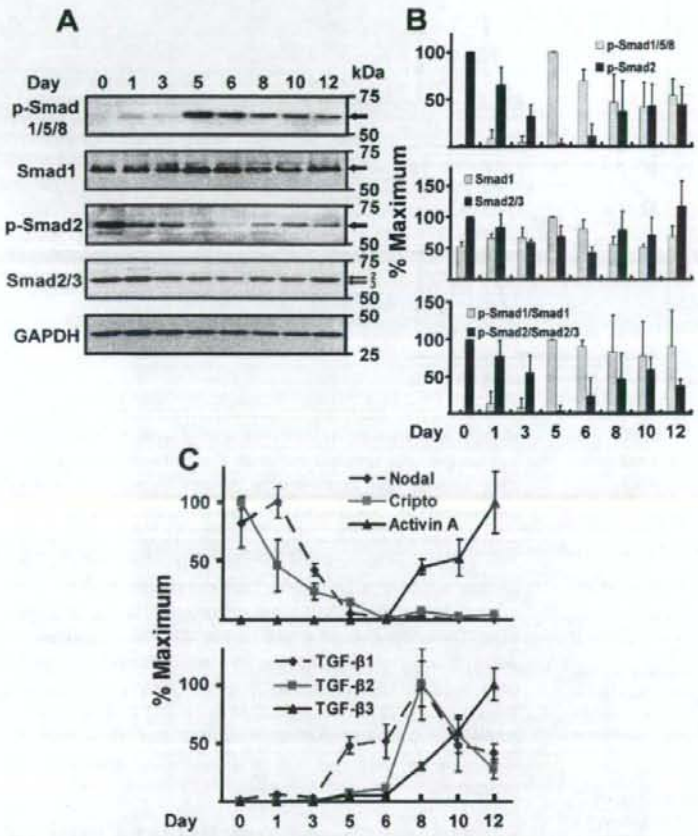

Figure 2. Activation of Smads and expression of TGF-βs, activin, Nodal, and Cripto during ES cell differentiation. A, Smads were analyzed by immunoblot analysis with the indicated antibodies. The corresponding bands are indicated with the arrows. B, Densitometric analysis was performed for Smads. The results are expressed as percentages of the maximum. C, Expression of Smad2-activating TGF-β family ligands Nodal, Cripto, activin, and TGF-βs was analyzed by real-time kinetic PCR. The results are expressed relative to the level of 18S ribosomal RNA and plotted as percentages of the maximum.

expression of TGF-β superfamily ligands, which can activate the Smad2 signaling pathway. Nodal and its coactivator Cripto were abundantly expressed in undifferentiated ES cells, whereas TGF-β and activin A were undetectable in these cells (Figure 2C). On induction of differentiation, the expression of Nodal and Cripto declined and was almost undetectable at day 5 (Figure 2C). In contrast, TGF-β and activin were markedly induced at days 5 and 8, respectively (Figure 2C). TGF-β isoforms showed different expression patterns during ES cell differentiation: the expression of TGF-β_1 and TGF-β_2 peaked at day 8 and then declined, whereas TGF-β_3 continued to be upregulated until day12 (Figure 2C). These results suggested that Smad2 was activated by Nodal/Cripto in the undifferentiated and early stages, whereas TGF-β and activin were responsible for the late activation of Smad2.

Smad2 Activation Has Stage-Specific Opposing Effects on Cardiomyogenesis in ES Cells

The role of Smad2 activation in cardiomyogenesis of ES cells was analyzed using SB-431542, a specific and potent inhibitor of ALK-4, -5, and -7.[11] To date, no target of SB-431542 other than Smad2-activating ALK-4, -5, and -7 has been reported, and SB-431542 has no effect on other ALK family members, extracellular signal-regulated kinase, c-Jun N-terminal kinase, or p38 mitogen-activated protein kinase at the concentration used in this study.[11] As Smad2 was activated biphasically in the early and late phases, cells were divided into 4 groups (Figure 3A): control; no treatment control, SB+/+; treated throughout differentiation, SB+/−; treated for only the first 5 days, SB−/+; treated after day 5. Treatment with SB-431542 completely abolished the phosphorylation of Smad2 throughout the course of differentiation (Figure 3C). Using ES cell clones that express EGFP under the transcriptional control of a cardiac-specific α-MHC promoter,[7] we examined the effects of phase-specific inhibition of Smad2 activation on cardiomyogenesis by analyzing the proportion of EGFP-positive cardiac myocytes (Figure 3A and 3B). When cells were treated in the early phase, cardiomyogenesis was markedly inhibited compared with the untreated control, although it was significantly augmented when cells were treated in only the late phase (Figure 3A). In untreated control cells, the proportion of cardiac myocytes was 4.1% (Figure 3B). On treatment with SB-431542 in the early phase, EGFP-positive cells decreased in a concentration-dependent manner, regardless of treatment in the late phase, and almost completely diminished at 5 μmol/L SB-431542 (Figure 3B). When treated in only the late phase,